AGU PUBLICATIONS

Geophysical Research Letters

RESEARCH LETTER
10.1002/2014GL062362

Key Points:
- Upper crustal anisotropy can be constrained by Rayleigh wave H/V ratios
- The upper crustal anisotropy across U.S. is determined using USArray data
- Clear correlation is observed between shallow anisotropy and a stress model

Supporting Information:
- Readme
- Figure S1

Correspondence to:
F.-C. Lin,
fanchi.lin@utah.edu

Citation:
Lin, F.-C., and B. Schmandt (2014), Upper crustal azimuthal anisotropy across the contiguous U.S. determined by Rayleigh wave ellipticity, *Geophys. Res. Lett.*, *41*, doi:10.1002/2014GL062362.

Received 28 OCT 2014
Accepted 17 NOV 2014
Accepted article online 20 NOV 2014

Upper crustal azimuthal anisotropy across the contiguous U.S. determined by Rayleigh wave ellipticity

Fan-Chi Lin[1] and Brandon Schmandt[2]

[1]Department of Geology and Geophysics, University of Utah, Salt Lake City, Utah, USA, [2]Department of Earth and Planetary Science, University of New Mexico, Albuquerque, New Mexico, USA

Abstract Constraints on upper crustal seismic anisotropy provide insight into the local stress orientation and structural fabric, but such constraints are scarce except in areas with dense recordings of local seismicity. We investigate directionally dependent Rayleigh wave ellipticity, or Rayleigh wave H/V (horizontal to vertical) amplitude ratios, between 8 and 20 s period across USArray to infer azimuthal anisotropy in the upper crust across the contiguous U.S. To determine the H/V ratios, we use all available multicomponent ambient noise cross correlations between all USArray stations operating between 2007 and 2013. In many locations, the observed H/V ratios are clearly back azimuth dependent with a 180° periodicity, which allows the fast directions and amplitudes of upper crustal anisotropy to be determined. The observed patterns of anisotropy correlate well with both near-surface geological features (e.g., the Intermountain Seismic Belt and Appalachian-Ouachita collision belt) and a previous stress model.

1. Introduction

Structural fabric and stress-induced microcrack alignment are often considered as the primary causes for upper crustal anisotropy [*Boness and Zoback*, 2006; *Crampin*, 1978; *Kern and Wenk*, 1990; *Aster and Shearer*, 1992; *Gerst and Savage*, 2004; *Sherrington et al*., 2004; *Yang et al*., 2011]. Traditional seismic methods often use shear wave splitting from local earthquakes to investigate shallow crustal anisotropy [*Crampin and Lovell*, 1991; *Savage*, 1999]. This approach is limited by the seismic source distribution and is not applicable in areas where seismicity is infrequent. The recent development of ambient noise tomography and the availability of passive data from industrial-type dense arrays provide an alternative way to study shallow crustal structure using high-frequency (~0.3–4 Hz) surface waves extracted from ambient noise [*Lin et al*., 2013; *Mordret et al*., 2013]. Such an approach is limited to very local scales, and continuous mapping of upper crustal anisotropy on regional or continental scales remains a challenge.

Recent studies on Rayleigh wave ellipticity provide a new approach to studying shallow Earth structure across larger scales using broadband arrays [*Yano et al*., 2009; *Lin et al*., 2012; *Tanimoto and Rivera*, 2008; *Tanimoto et al*., 2013; *Lin et al*., 2012, 2014]. Rayleigh wave ellipticity, described by the Rayleigh wave horizontal to vertical amplitude ratio (H/V ratio), is a site property with significant shallow sensitivity (Figure 1) [*Boore and Toksöz*, 1969; *Tanimoto and Rivera*, 2008]. Different from the traditional noise spectral H/V ratio [*Bonnefoy-Claudet et al*., 2006], the Rayleigh wave H/V ratio can be theoretically determined for a 1-D Earth model using the Rayleigh wave radial and vertical eigenfunctions [*Tanimoto and Rivera*, 2008]. Studying Rayleigh wave H/V ratios using either earthquake signals or ambient noise cross correlations has led to improved crustal models in both Southern California and other parts of the western U.S. [*Lin et al*., 2012, 2014; *Tanimoto et al*., 2013]. Throughout this manuscript, we sometimes refer to the Rayleigh wave H/V ratio as "the H/V ratio" for conciseness, but the term should not be confused with the traditional noise spectral H/V ratio.

In this study, we explore the possibility of studying upper crustal anisotropy across the contiguous U.S. using the directionally dependent Rayleigh wave H/V ratio measurements. Similar to Rayleigh wave phase velocities, Rayleigh wave H/V ratios are sensitive to azimuthal anisotropy of shear wave velocity [*Tanimoto and Rivera*, 2008], and like isotropic H/V ratios, such sensitivity is extremely shallow, which allows upper crustal anisotropy to be constrained. Here following our previous Rayleigh wave H/V ratio study with multicomponent ambient noise cross correlations in the western U.S. [*Lin et al*., 2014], we first expand

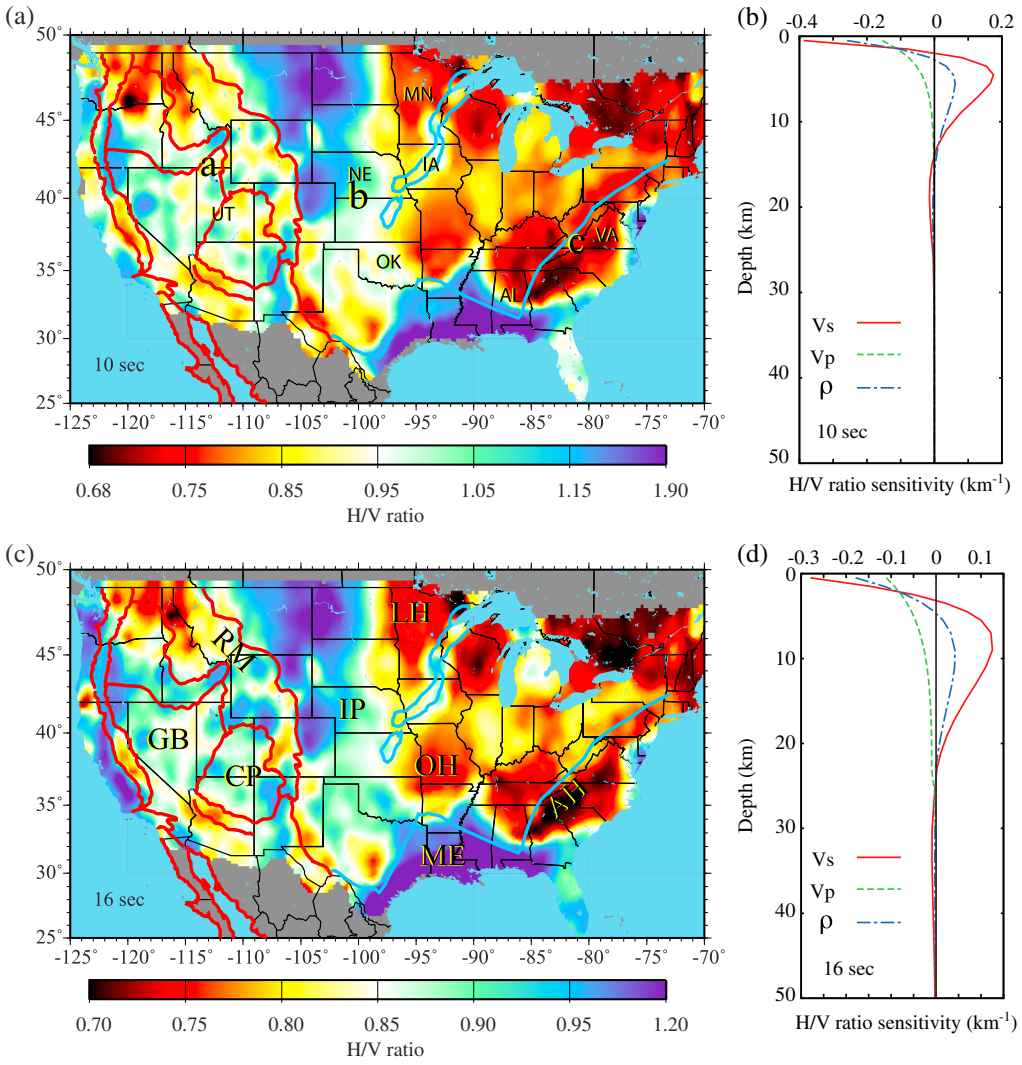

Figure 1. (a) The 10 s Rayleigh wave H/V ratio observed across USArray. The letters a, b, and c indicate the example locations used in Figure 2. The red contours denote the tectonic boundaries in the western U.S. The blue contour denotes the approximate locations of the Midcontinent Rift and the Precambrian Rift Margins in the eastern U.S [*Whitmeyer and Karlstrom*, 2007]. Several states mentioned in the text are also identified. UT: Utah; NE: Nebraska; OK: Oklahoma; MN: Minnesota; IA: Iowa; AL: Alabama; and VA: Virginia. (b) The depth sensitivities of the 10 s H/V ratio to *Vs*, *Vp*, and density (ρ). (c, d) Same as Figures 1a and 1b but for the 16 s H/V ratio. GB: Great Basin; CP: Colorado Plateau; RM: Rocky Mountains; IP: Interior Plain Province; EM: Mississippi embayment; LH: Laurentian Highlands; OH: Ouachita-Ozark Interior Highlands; and AH: Appalachian Highlands.

our data coverage to include most of the contiguous U.S. and then analyze the azimuthal dependence of Rayleigh wave H/V ratio measurements. Clear anisotropy signals are identified based on observations of 180° periodicity in the H/V ratio. The resulting map of inferred upper crustal anisotropy correlates well with known geological structures and the stress field in North America previously inferred from independent measurements [*Heidbach et al.*, 2010].

2. Data and Results

We closely follow the method described by *Lin et al.* [2014] to obtain 8 to 20 s Rayleigh wave H/V ratio measurements across USArray. First, all available three-component ambient noise records between 1 January 2007 and 31 December 2013 are used to compute ZZ, ZR, RZ, and RR (*Z* and *R* represent vertical and radial components, respectively) noise cross correlations between all stations [*Bensen et al.*, 2007; *Lin et al.*, 2008].

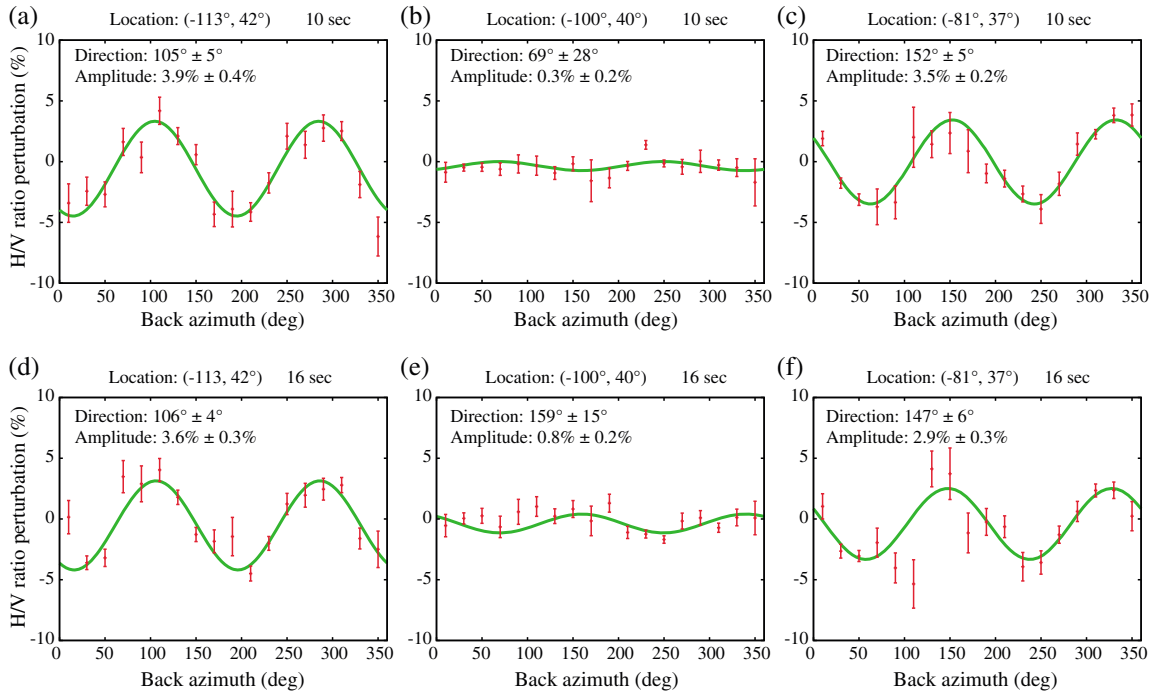

Figure 2. (a–c) Examples of 10 s directionally dependent Rayleigh wave H/V ratio perturbations at the locations denoted in Figure 1a. The red bars represent the mean perturbations and their uncertainties in each 20° azimuthal bin relative to the isotropic H/V ratio. For each case, the solid green line is the best fit of the 180° periodicity azimuthal variation. The high H/V ratio direction and the variation amplitude of the fit are also shown. (d–f) Same as Figures 2a–2c but for the 16 s period.

Simultaneous temporal and spectral normalization of each component's noise time series is performed prior to cross correlation to ensure that the amplitude ratio information between different components is not lost [*Lin et al.*, 2014]. For each station pair, the amplitude ratios between different component cross correlations are then used to determine Rayleigh wave H/V ratios at the two station locations, considering one station as a virtual source and the other as a receiver. The Rayleigh wave H/V ratios derived from different virtual sources but at the same receiver location are averaged to obtain the isotropic H/V ratio. Back azimuth dependence of the H/V ratio at the receiver location is identified by binning the virtual sources in 20° increments, where the back azimuth direction of each measurement is determined by the great circle path connecting the virtual source to the receiver. Examples of raw directionally dependent H/V ratio measurements before averaging and stacking can be found in Figure S1 in the supporting information.

Figure 1 summarizes the 10 and 16 s period Rayleigh wave isotropic H/V ratios observed across USArray. Here a 0.5° Gaussian smoothing is applied to interpolate the result from station locations to a 0.2° × 0.2° grid (Figures 1a and 1c). At these periods, the H/V ratios are most sensitive to upper crustal structure. High H/V ratios typically represent strong positive velocity gradients in the upper crust, such as sedimentary basins overlying relatively high velocity bedrock. Low H/V ratios typically represent weak velocity gradients in the upper crust, which are common where high-velocity bedrock is reached at very shallow depths or outcrops at the surface. In the western U.S., the results are consistent with our prior study [*Lin et al.*, 2014], with high H/V ratios observed in major sedimentary basins and low H/V ratios observed in major mountain ranges. In the east, extremely high H/V ratios are observed in the Mississippi embayment where thick sediments are present [*Laske and Masters*, 1997]. Slightly higher than average H/V ratios are also observed in the midcontinental rift, likely related to the shallow sediments in the failed rift system [*Hinze et al.*, 1992; *Shen et al.*, 2013]. Low H/V ratios are observed in areas where deeply exhumed bedrock outcrops at the surface including the Laurentian Highlands, the Ouachita-Ozark Interior Highlands, and the Appalachian Highlands. A 3-D inversion integrating other types of surface wave dispersion measurements [e.g., *Lin et al.*, 2012, 2014] will be the subject of future studies. Here we focus on investigation of azimuthal anisotropy in H/V ratios extracted from ambient noise.

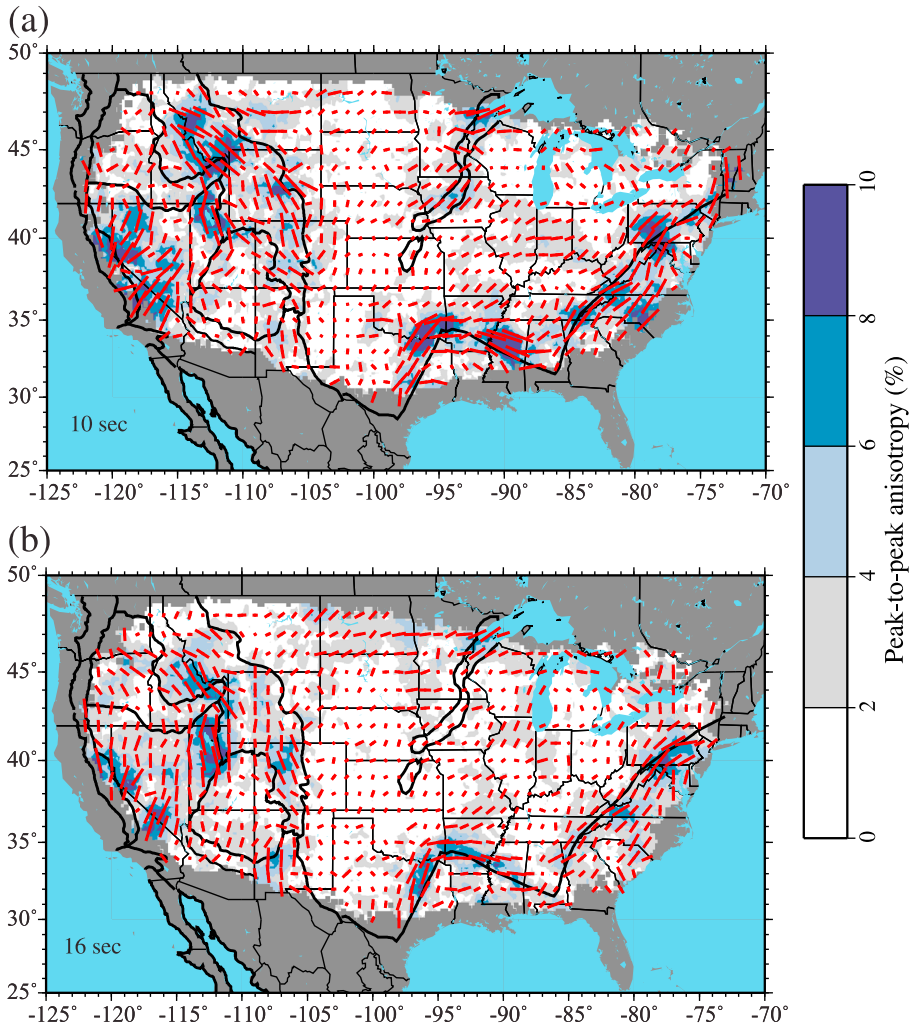

Figure 3. (a) The azimuthal anisotropy of the 10 s period Rayleigh wave H/V ratio. The red bars indicate the low H/V ratio directions (or the inferred upper crustal fast directions). The lengths of the bars are proportional to the peak-to-peak amplitudes, which are also shown by the background color. (b) Same as Figure 3a but for the 16 s period.

For each station and period, we remove the isotropic H/V ratio from each H/V ratio measurement to isolate directionally dependent variations. For each location all measurements from stations within 100 km are used in order to boost the signal-to-noise ratio. Measurements within each 20° back azimuth bin are summarized to calculate the averaged H/V ratio perturbation and its uncertainty. Figure 2 shows the observed directionally dependent H/V ratio variations for the 10 and 16 s period Rayleigh waves at three distinct geological locations. In northern Utah and southwestern Virginia clear 180° periodicity in the H/V ratio is observed, which is a signature of an azimuthally anisotropic medium [*Smith and Dahlen*, 1973]. Both stations exhibit anisotropic H/V ratios with peak-to-peak amplitudes of ~7%. In contrast, the third example station located in southern Nebraska does not exhibit a robust anisotropic signal, which suggests that the upper crustal structure in this location within the Interior Plains Province is mostly isotropic.

Wherever a clear anisotropy pattern is observed, the directionally dependent H/V ratio measurements allow us to determine the high and low H/V ratio directions and anisotropy amplitude based on least squares fitting. Previous azimuthal anisotropy studies across USArray based on Rayleigh wave phase velocity measurements suggest that anisotropy in the middle/lower crust is normally smaller than 2% [*Lin et al.*, 2009, 2011]. Regional upper crustal anisotropy studies, on the other hand, suggest that the uppermost crust can be significantly anisotropic with amplitudes larger than 10% in some cases [*Lin et al.*, 2013; *Crampin*, 1994].

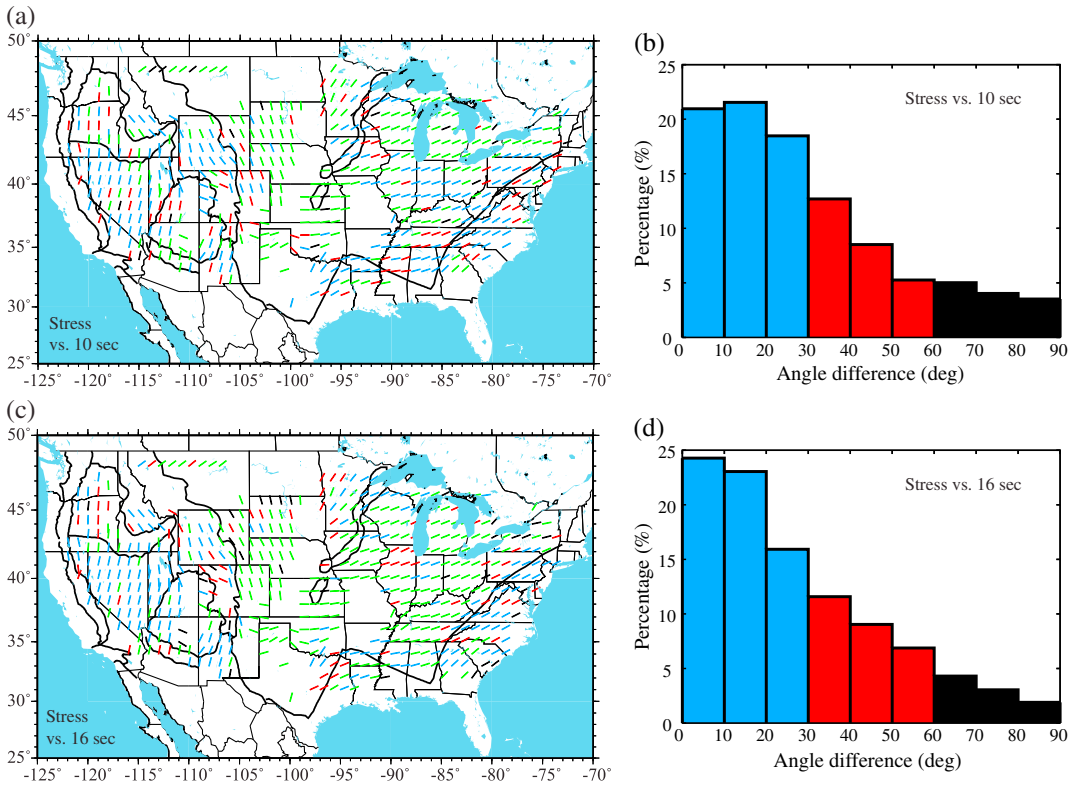

Figure 4. The comparison between the maximum compressive stress directions and the inferred upper crustal fast directions. (a) The colored bars show the maximum compressive stress axes modeled by *Heidbach et al.* [2010]. The blue, red, and black colors identify angle differences between the stress direction and the fast direction inferred by 10 s H/V ratio anisotropy: blue: 0°–30°, red: 30°–60°, and black: 60°–90°. The green color identifies locations with observed anisotropy amplitudes smaller than 2%, where the fast directions cannot be robustly determined. (b) The distribution of angle differences between the compressive stress direction and fast direction inferred by 10 s H/V ratio anisotropy. (c, d) Same as Figures 4a and 4b but for 16 s H/V ratio anisotropy.

These earlier observations suggest that the strong anisotropy signals (Figures 2a, 2c, 2d, and 2f) observed for the H/V ratios are most likely related to anisotropic structure in the uppermost crust.

We assume that the strength of azimuthal anisotropy amplitude decreases rapidly with depth and the observed H/V ratio anisotropy is mostly related to the azimuthal anisotropy in the top ~3 km. Figure 3 summarizes the observed 10 and 16 s period Rayleigh wave H/V ratio azimuthal anisotropy and the inferred upper crustal fast directions across the contiguous U.S. Here we remove all locations with more than a 120° back azimuth gap in the H/V ratio measurements to retain only the most robust measurements. This, however, also removes all locations near the edges of USArray. Overall, the observed anisotropy patterns are very similar for the two periods, consistent with the shallow anisotropy assumption, as both periods are strongly sensitive to the uppermost crustal structure (Figures 1b and 1d).

3. Discussion

In the western U.S., anisotropy with amplitude >2% is observed in most geological provinces except the Colorado Plateau. In the Great Basin, persistent north-south fast directions are observed at the 16 s period, which are likely related to the north-south basin and range alignment and the principal east-west extensional stress [*Flesch et al.*, 2000]. The anisotropy is particularly strong on the eastern edge of the Great Basin, where higher than 8% anisotropy is observed in both the 10 and 16 s periods and the north-south fast directions are aligned with the Intermountain Seismic Belt [*Smith and Sbar*, 1974]. Strong anisotropy is also observed in the Northern and Southern Rockies where fast directions are subparallel to the Rocky Mountain Front.

In the eastern U.S., a striking correlation is observed between the anisotropy pattern and the inferred Precambrian Rift Margins that parallel the Appalachian-Ouachita ancient collision belt [*Whitmeyer and Karlstrom*, 2007]. Strong anisotropy (>6%) is observed in both the 10 and 16 s periods with fast directions well aligned with the strike of major mountain ranges. Intriguingly, the anisotropy fast directions rotate ~90° at both southern Alabama and southeastern Oklahoma, closely following the inferred orientation change of the Precambrian Rift Margin [*Whitmeyer and Karlstrom*, 2007]. Different from the isotropic H/V ratio pattern observed (Figure 1), the anisotropy pattern follows the Precambrian Rift Margin across the Mississippi embayment, and hence, it is not simply correlated with thick sedimentary deposits. Away from the ancient rift margins, weak to negligible anisotropy is observed across the cratonic interior except in the area of the Midcontinental Rift. Intermediate-amplitude anisotropy (~4%) is observed at the 10 s period near the Midcontinental Rift in Iowa and Minnesota with the fast direction subparallel to the rift system. At the same location, negligible anisotropy is observed at the 16 s period, however, suggesting the anisotropic structure associated with the Midcontinental Rift system may change significantly over small changes in depth.

Distinguishing between the effects of stress-induced microcrack alignment and structural fabric (e.g., foliation) on observations of H/V ratio anisotropy can be difficult. In particular, major geological features often align with the principal stress direction (such as the Basin and Range Province), and the gravitational potential energy variations associated with major geological features can also induce regional deviatoric stress [*Jones et al*., 1996; *Flesch et al*., 2000]. When the stress field is not hydrostatic, microcracks aligned with the maximum compressive principal axis will close preferentially and seismic waves will propagate faster along the same direction [*Crampin and Lovell*, 1991]. To investigate whether the observed H/V ratio anisotropy can be explained by stress-induced microcrack alignment and potentially be used to map the continental stress field with ambient seismic noise, we compare our inferred fast H/V ratio directions with the smoothed stress model of *Heidbach et al*. [2010]. The model was derived based on the compilation of stress indicators, which are primarily consistent of earthquake focal mechanisms and well bore breakouts [*Heidbach et al*., 2008].

A clear correlation is observed between the maximum compressive directions of *Heidbach et al*. [2010] and our inferred fast directions for both the 10 and 16 s period H/V ratios across the contiguous U.S. (Figure 4). For comparison with the stress model we use only the H/V ratio fast directions with anisotropy amplitudes >2%. For locations with a reliable fast direction and where the stress model is available, the fast direction is aligned within 30° of the maximum compressive direction for more than 60% of the locations (Figures 4b and 4d). This correlation is significant considering that the anisotropy observation and the stress model have a very different lateral resolution and depth sensitivity. Depending on the area, the stress model has a lateral resolution ranging between 100 and 1000 km [*Heidbach et al*., 2010] where the resolution of the anisotropy measurements is ~200 km everywhere due to the 100 km radius station averaging performed. Strong correlations of the two directions are observed in areas such as the Great Basin, Rocky Mountains, and Appalachian Ranges. Weak correlation areas, on the other hand, are relatively scattered and potentially due to resolution mismatch.

The 180° periodicity of directionally dependent H/V ratio measurements along with correlations between the inferred anisotropy pattern and major geological features and an independently derived stress model demonstrate the utility of measuring H/V anisotropy for studying the upper crust. The 3-D anisotropic structure of the lithosphere could be resolved over a broader depth interval by exploiting the complementary sensitivities of the H/V ratio and traditional measurements of anisotropic Rayleigh wave phase velocities [e.g., *Lin et al*., 2011]. Investigations of upper crustal anisotropy where the structural fabric and maximum compressive stress are not aligned will help determine the dominant factor controlling shallow crustal anisotropy. Alaska, for example, with major mountain ranges perpendicular to the maximum compressive stress direction, is an ideal area and will soon be covered by the ongoing USArray deployment. Our present results spanning most of the contiguous U.S. suggest that H/V ratio anisotropy is strongly influenced by the direction of maximum compressive stress in the shallow crust.

Acknowledgments

The authors thank two anonymous reviewers for comments that helped to improve this paper. Instruments (data) used in this study were made available through EarthScope (EAR-0323309), supported by the National Science Foundation. The facilities of the IRIS Data Management System (EAR-0552316) were used to access the waveform and metadata required in this study. F. Lin acknowledges the support from University of Utah and a grant from the U.S. National Science Foundation, CyberSEES-1442665, for this research.

The Editor thanks two anonymous reviewers for their assistance in evaluating this paper.

References

Aster, R. C., and P. M. Shearer (1992), Initial shear wave particle motions and stress constraints at the Anza Seismic Network, *Geophys. J. Int.*, *108*, 740–748, doi:10.1111/j.1365-246X.1992.tb03465.x.

Bensen, G. D., M. H. Ritzwoller, M. P. Barmin, A. L. Levshin, F. Lin, M. P. Moschetti, N. M. Shapiro, and Y. Yang (2007), Processing seismic ambient noise data to obtain reliable broad-band surface wave dispersion measurements, *Geophys. J. Int.*, *169*, 1239–1260, doi:10.1111/j.1365-246X.2007.03374.x.

Boness, N. L., and M. D. Zoback (2006), A multiscale study of the mechanisms controlling shear velocity anisotropy in the San Andreas Fault Observatory at Depth, *Geophysics*, *71*(5), doi:10.1190/1.2231107.
Bonnefoy-Claudet, S., F. Cotton, and P.-Y. Bard (2006), The nature of the seismic noise wave field and its implication for site effects studies: A literature review, *Earth Sci. Rev.*, *79*(3–4), 205–227.
Boore, D., and M. N. Toksöz (1969), Rayleigh wave particle motion and crustal structure, *Bull. Seismol. Soc. Am.*, *59*, 331–346.
Crampin, S. (1978), Seismic-wave propagation through a cracked solid: Polarization as a possible dilatancy diagnostic, *Geophys. J. R. Astron. Soc.*, *53*, 467–496.
Crampin, S. (1994), The fracture criticality of crustal rocks, *Geophys. J. Int.*, *118*, 428–438, doi:10.1111/j.1365-246X.1994.tb03974.x.
Crampin, S., and J. H. Lovell (1991), A decade of shear-wave splitting in the Earth's crust: What does it mean? What use can we make of it? And what should we do next?, *Geophys. J. Int.*, *107*, 387–407.
Flesch, L. . M., W. . E. Holt, A. . J. Haines, and B. Shen-Tu (2000), Dynamics of the Pacific-North American plate boundary in the western United States, *Science*, *834*, 834–836, doi:10.1126/science.287.5454.834.
Gerst, A., and M. K. Savage (2004), Seismic anisotropy beneath Ruapehu volcano: A possible eruption forecasting tool, *Science*, *306*(5701), 1543–1547.
Heidbach, O., M. Tingay, A. Barth, J. Reinecker, D. Kurfeß, and B. Müller (2008), The World Stress Map database release 2008 doi:10.1594/GFZ.WSM.Rel2008. [Available at http://dc-app3-14.gfz-potsdam.de/pub/stress_maps/stress_maps.html.]
Heidbach, O., M. Tingay, A. Barth, J. Reinecker, D. Kurfeß, and B. Müller (2010), Global crustal stress pattern based on the World Stress Map database release 2008, *Tectonophysics*, *462*, doi:10.1016/j.tecto.2009.1007.1023.
Hinze, W. J., D. J. Allen, A. J. Fox, D. Sunwood, T. Woelk, and A. G. Green (1992), Geophysical investigations and crustal structure of the North American Midcontinent Rift system, *Tectonophysics*, *213*(1–2), 17–32, doi:10.1016/0040-1951(92)90248-5.
Jones, C. H., J. Unruh, and L. J. Sonder (1996), The role of gravitational potential energy in active deformation in the southwestern United States, *Nature*, *381*, 37–41.
Kern, H., and H.-. R. Wenk (1990), Fabric-related velocity anisotropy and shear wave splitting in rocks from the Santa Rosa Mylonite Zone, California, *J. Geophys. Res.*, *95*, 11,213–11,223, doi:10.1029/JB095iB07p11213.
Laske, G., and G. Masters (1997), A global digital map of sediment thickness, *Eos Trans. AGU*, *78*, 483.
Lin, F.-C., M. P. Moschetti, and M. H. Ritzwoller (2008), Surface wave tomography of the western United States from ambient seismic noise: Rayleigh and Love wave phase velocity maps, *Geophys. J. Int.*, *173*, 281–198, doi:10.1111/j.1365-246X.2008.03720.x.
Lin, F.-C., M. H. Ritzwoller, and R. Snieder (2009), Eikonal tomography: Surface wave tomography by phase front tracking across a regional broad-band seismic array, *Geophys. J. Int.*, *177*, 1091–1110, doi:10.1111/j.1365-246X.2009.04105.x.
Lin, F.-C., M. H. Ritzwoller, Y. Yang, M. P. Moschetti, and M. J. Fouch (2011), Complex and variable crustal and uppermost mantle seismic anisotropy in the western United States, *Nat. Geosci.*, *4*, 55–61, doi:10.1038/ngeo1036.
Lin, F.-C., B. Schmandt, and V. C. Tsai (2012), Joint inversion of Rayleigh wave phase velocity and ellipticity using USArray: Constraining velocity and density structure in the upper crust, *Geophys. Res. Lett.*, *39*, L12303, doi:10.1029/2012GL052196.
Lin, F.-C., D. Li, R. W. Clayton, and D. Hollis (2013), High-resolution 3D shallow crustal structure in Long Beach, California: Application of ambient noise tomography on a dense seismic array, *Geophysics*, *78*(4), Q45–Q56, doi:10.1190/geo2012-0453.1.
Lin, F.-C., V. C. Tsai, and B. Schmandt (2014), 3-D crustal structure of the western United States: Application of Rayleigh-wave ellipticity extracted from noise cross-correlations, *Geophys. J. Int*, *198*(2), 656–670, doi:10.1093/gji/ggu160.
Mordret, A., N. M. Shapiro, S. Singh, P. Roux, J.-P. Montagner, and O. I. Barkved (2013), Azimuthal anisotropy at Valhall: The Helmholtz equation approach, *Geophys. Res. Lett.*, *40*, 2636–2641, doi:10.1002/grl.50447.
Savage, M. K. (1999), Seismic anisotropy and mantle deformation: What have we learned from shear wave splitting?, *Rev. Geophys.*, *37*(1), 65–106, doi:10.1029/98RG02075.
Shen, W., M. H. Ritzwoller, and V. Schulte-Pelkum (2013), Crustal and uppermost mantle structure in the central U.S. encompassing the Midcontinent Rift, *J. Geophys. Res. Solid Earth*, *118*, 4325–4344, doi:10.1002/jgrb.50321.
Sherrington, H. F., G. Zandt, and A. Frederiksen (2004), Crustal fabric in the Tibetan Plateau based on waveform inversions for seismic anisotropy parameters, *J. Geophys. Res.*, *109*, B02312, doi:10.1029/2002JB002345.
Smith, M. L., and F. A. Dahlen (1973), Azimuthal dependence of Love and Rayleigh wave propagation in a slightly anisotropic medium, *J. Geophys. Res.*, *78*, 3321–3333, doi:10.1029/JB078i017p03321.
Smith, R. B., and M. L. Sbar (1974), Contemporary tectonics and seismicity of the western United States with emphasis on the Intermountain Seismic Belt, *Geol. Soc. Am. Bull.*, *85.8*(197), 1205–1218.
Tanimoto, T., and L. Rivera (2008), The ZH ratio method for long-period seismic data: Sensitivity kernels and observational techniques, *Geophys. J. Int.*, *172*, 187–198, doi:10.1111/j.1365-246X.2007.03609.x.
Tanimoto, T., T. Yano, and T. Hakamata (2013), An approach to improve Rayleigh-wave ellipticity estimates from seismic noise: Application to the Los Angeles Basin, *Geophys. J. Int.*, *193*(1), 407–420.
Whitmeyer, S. J., and K. E. Karlstrom (2007), Tectonic model for the Proterozoic growth of North America, *Geosphere*, *3*(4), 220–259, doi:10.1130/ges00055.1.
Yang, Z., A. Sheehan, and P. Shearer (2011), Stress-induced upper crustal anisotropy in southern California, *J. Geophys. Res.*, *116*, B02302, doi:10.1029/2010JB007655.
Yano, T., T. Tanimoto, and L. Rivera (2009), The ZH ratio method for long-period seismic data: Inversion for *S*-wave velocity structure, *Geophys. J. Int.*, *179*, 413–424, doi:10.1111/j.1365-246X.2009.04293.x.